

proposed. It is compared with other methods which have other combinations of features using different windows. The Most Confident SML approach performs the best.

**Acknowledgement:**

We would like to express our gratitude to Dr. K. C. Lee of Prince Margaret Hospital in Hong Kong for his invaluable advice and help, as well as to Hong Kong Jockey Club Charities Trust for its financial support in the project.

**References:**

- [1] A. K. Jain and F. Farrottoia, "Unsupervised Texture Segmentation Using Gabor Filters", *Pattern Recognition*, vol. 24, no. 12, pp. 1167-1185, 1991.
- [2] T. Kondo and J. H. Huidy, "Filtering for Image Classification - A Comparative Study", *IEEE Trans. Pattern Anal. & Machine Intel.*, vol. 4, pp. 291 - 310, 1982.
- [3] D. S. Margolis, and W. T. Ma, "Texture Filtering, Thresholding and Retrieval of Image Data", *IEEE Trans. Pattern Anal. & Machine Intel.*, vol. 11, no. 4, 1989, pp. 437 - 442.
- [4] P. Brodat, *Textures - A Photographic Approach for Artists & Designers*, New York: Dover, 1956.

# International Conference on Pattern Recognition

September 3-7

Volume 2  
Pattern Recognition and Neural Networks

Editors:  
A. Sanfeliu  
J.J. Villanueva  
M. Vanrell  
R. Alquézar  
A.K. Jain  
J. Kittler

Table 3 Accuracy rates of the 10-fold method



# Abdominal Organ Recognition using 3D Mathematical Morphology

Toyohisa Kaneko, Lixu Gu, and Hideyuki Fujimoto

Toyohashi University of Technology

1-1 Hibarigaoka, Tempaku-cho, Toyohashi 441-8580, Japan

{kaneko}@tutics.tut.ac.jp

## Abstract

We describe a method for automatic recognition of abdominal organs such as kidneys, spleen, stomach, and liver from computing tomography (CT) images using three-dimensional (3D) mathematical morphology. Morphological approaches provide the theory and tools to analyze shapes directly. This characteristic enables analyzing and recognizing abdominal organs according to size and gray level features. Our system consists of extraction part and recognition part. Differential top-hats (DTT) and conditional dilation are used for the extraction part. Also a combination of recursive erosion and geodesic influence is found to be effective for separating touched organs. Recognition is based on a simple likelihood decision with organ's position and size. We obtained a recognition rate of about 91% for nine organs of four CT images.

## 1. Introduction

This paper is concerned with automatic recognition of abdominal organs such as kidneys, spleen, stomach, and liver from CT. Most of the past organ extraction and recognition approaches are not only involving many manual operations, but also using some organ specific algorithms, such as region growing [1] and skeleton method [2, 3]. In this paper, we describe a new method for automatically recognizing many (actually up to nine) abdominal organs at once or in parallel from CT images primarily using 3D mathematical morphology. These results are useful for executing organ specific cancer detection algorithms, for example, and for surgery simulation where individual organs must be separately treated and modeled.

The entire procedure consists of two steps: extraction and recognition processing. In the first processing, we use a new morphological segmentation algorithm called DTT[5, 6] which was derived from top-hats and

morphological recursive operation. It is applied to extracting candidate organ regions from CT data. Then the next step is the recognition of organs based upon morphological operations for dividing touched organs and statistics of organ positions and sizes.

The organization of this paper is as follows. Section 2 is a brief overview of 3D morphological operations such as conditional dilation and top-hats. Section 3 and 4 describe the details of our organ extraction and recognition, respectively. Experiments are discussed in section 5, and conclusion is in section 6.

## 2. 3D Morphology

The 3D morphology is derived from 2D theory. It also include 3D Dilation, Erosion, Opening, and Closing. In the following we will describe some important operations utilized in this paper.

### 2.1. Conditional Dilation

As shown in Figure 1, conditional dilation,  $R_i(V, M)$ , is an operation for enlarging a region  $M$  called a 'marker' within a boundary  $V$  called a 'mask' where  $M \subseteq V$ . This operation is defined as:

$$R_i(V, M) = (M \oplus^i K) \cap V, \quad (1)$$

where  $i$  is the minimum integer to satisfy:

$$R_i(V, M) = R_{i-1}(V, M). \quad (2)$$

### 2.2. Top-hats

This operation[4] extracts a region near the top of an input image within a given structure element. Let  $T_i$  represent the extracted region. Then the following defines this operation.

$$T_i = F_0 - F_0 \circ_g r_i K \quad (3)$$

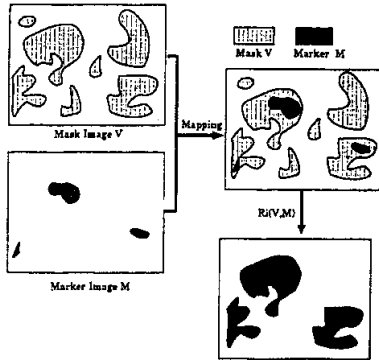


Figure 1: Binary reconstruction - conditional dilation

Here,  $F_0$  is the original gray-scale image and  $K$  is the structure element. And  $r_i K$  is defined as:  $r_i K = K \oplus K \oplus \dots \oplus K$  ( $r_i$  times).

### 2.3 Differential Top-hats

This is an improved version[5, 6] of Top-hats which takes a consecutive difference with varying the structure element size (see Equation 6).

### 2.4 Recursive Erosion

The recursive erosion is defined as:

$$F \ominus^i K = \begin{cases} F & \text{if } i = 0 \\ (F \ominus^{i-1} K) \ominus K & \text{if } i \geq 1 \end{cases} \quad (4)$$

As shown in Figure 2, this operation divides a region  $F$  into a set of subregions by repeating  $i$  times where  $i$  is the number of times just before any of the seeds ( $S_1 \sim S_n$ ) disappears.

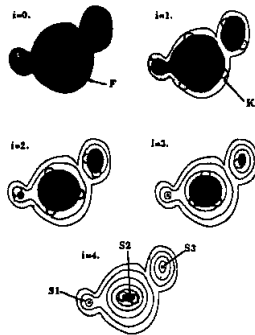


Figure 2: Recursive erosion

### 2.5 Pattern Spectrum

Let  $F$  be the input, and  $r_n K$  be the structure element. Then Pattern Spectrum ( $PS_n$ ) is defined as:

$$\begin{aligned} F_{nB} &= F \circ r_n K \\ PS_n &= F_{nB} - F_{(n+1)B} \\ &\text{if } F_{nB} = \phi \text{ then stop} \end{aligned} \quad (5)$$

Pattern Spectrum enables us to estimate a distribution in sizes like power spectrum which provides a distribution in frequency.

### 3 Extraction

DTT (see 2.3)) is operated on input CT data to provide 3D organ candidate regions to which conditional dilation (see 2.1) is applied to include the abdominal organ regions as correctly as possible. More detailed description is as follows.

To get organ candidate regions, we place, in bright regions in CT, structure elements shown in Fig.3 whose sizes or radii are incremented by 1 with the starting size of 1. We take a consecutive difference and the resulting difference is binarized with a threshold value which is experimentally determined (see section 5). This operation is described in the following morphological operations.

Let  $F_0$  be the input CT data. The intermediate results  $F_i$  are operated by opening with structure element ( $r_{(i-2)} K_{sphere}$ ) as:

$$\begin{aligned} F_i &= |T_i - T_{i-1}|_B - F'_{i-1} \\ F'_i &= \bigcup_{1 \leq j \leq i} (F_j \circ r_{(j-2)} K_{sphere}) \\ F'_1 &= \emptyset \\ T_i &= F_0 - F_0 \circ_g r_i K_{sphere} \\ &\text{if } F'_i = F'_{i-1} \text{ then stop} \end{aligned} \quad (6)$$

where  $r_i K_{sphere}$  is a spherical structure element with radius  $i$  and  $|_B$  is an threshold operation. The final result becomes  $F'_n$ , where  $n = 26$  is chosen for this experiment (see section 5).

### 4 Recognition

The extracted organs are to be labeled or recognized. We use location or position information for labeling.

#### 4.1 The Coordinate System

We set up a coordinate system and its origin in order to specify an abdominal position and size. All the CT



Figure 3: Examples of structure elements( $r=2,3$ )

data (provided by the National Cancer Center) include several lower ribs. So we decided that the coordinate origin is set at the center point of the 12th thoracic vertebra to which the lowest rib joins. The x-y plain is along the CT cross section. And the z-direction is set to be positive toward downward along its axial direction.

#### 4.2 Normalization

Organ sizes are dependent on people so that we need normalization to measure organ sizes of different people. We decided to use the average distance between the successive vertebrae for normalization. Actually the total difference from the center of 11th thoracic vertebra to that of the fourth lumbar vertebra is set to be a unit of 1. Similarly the total width and the total depth along the x-y direction along the section at the origin is set to be a unit of 1.

#### 4.3 Separation of Touched Organs

We found that the left kidney, spleen, and stomach are often touched or stucked, requiring a separation process. Here we found that a combination of two morphological operations, recursive erosion (RE) and geodesic influence (GI) is very effective. This is illustrated in Fig.4. Fig.4(a) shows three touched organs. The recursive erosion provides Fig.4(b). Then the process is reversed as is shown in Fig.4(c) to provide the final result of Fig.4(d), where the dividing borders are the equi-distance lines generated by the three seed centers shown in Fig.4(b). In general if touched organs are convex, the combination of RE and GI is effective in their separation.

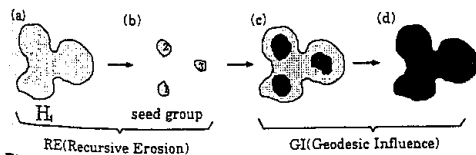


Figure 4: Separation of left kidney, spleen, and stomach

## 5 Experiments

### 5.1 CT Data

We used four CT data provided by the National Cancer Center, East Hospital. These were acquired for diagnosing possible cancer patients. Dye was injected to the vein (vena cava) several minutes before the initiation of the CT instrument. The CT data have a resolution of 512x512, where pixel-to-pixel distance is .625[mm] and slice distance is 2[mm]. The numbers of slices are 103, 94, 102, and 104 for CT data #1 to #4. Two new slices with linear interpolation were inserted between two successive CT slices to have an approximately cubic voxel.

### 5.2 Organ Geometry Statistics

We will illustrate the recognition process of three abdominal organs, left kidney, and stomach which tend to be stucked, as was mentioned earlier. We gathered statistics for these organs. Table 1 lists sizes of left kidney, spleen, and stomach, while Table 2 lists positions of the gravity center of these organs. These data were obtained by manual identification of these organs for each slice of the four CT data. Then for each measurement we computed the average  $\mu$  and standard deviation  $\sigma$ .

### 5.3 Extraction

For organ extraction, we varied the spherical structure radius from 1 to 26 (the radius of 26 corresponds to .625[mm]x26=1.6[cm]). All the intermediate results were binarized with a threshold. The final result is given as their union. The threshold was set to be 10 in the gray scale of 0 to 255. This value was applicable to all the four CT data. Fig.5 shows one of the results. The figure, which shows a back view and a top view, was made by applying the marching cubes algorithm to the final binary image. By comparing the automatically extracted regions with the manually extracted regions, we obtained accuracy of about 95%.

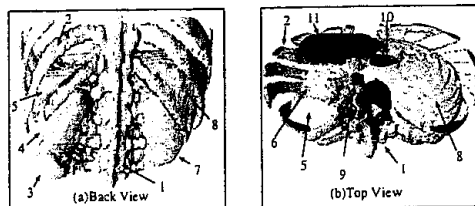


Figure 5: Extraction Result CT#2  
 (1.Column 2.Rib 3.Pelvis 4.Left Kidney 5.Spleen  
 6.Stomach 7.Right Kidney 8.Liver 9.Pulmonary vein  
 10.Vena Cava 11.Heart)

### 5.4 Recognition

Table 1: Size of left kidney(LK), spleen(SP), and stomach(ST)

CT	LK	SP	ST
#1	1.1	1.4	-
#2	1.1	1.5	2.9
#3	1.1	1.6	3.6
#4	-	1.6	-
$\mu$	1.1	1.50	3.2
$\sigma$	0.04	0.10	0.40

Table 2: Position of left kidney, spleen, and stomach

CT	LK			Spleen			Stomach		
	x	y	z	x	y	z	x	y	z
#1	0.14	-0.23	0.64	0.10	-0.34	0.28	-	-	-
#2	0.16	-0.29	0.63	0.14	-0.32	0.38	0.51	-0.25	0.60
#3	0.14	-0.25	0.62	0.09	-0.32	0.23	0.47	-0.26	0.50
#4	-	-	-	0.08	-0.27	0.26	-	-	-
$\mu$	0.14	-0.25	0.63	0.10	-0.31	0.29	0.49	-0.25	0.54
$\sigma$	0.017	0.042	0.033	0.061	0.063	0.11	0.028	0.008	0.066

Abdominal organs are mutually connected through veins and arteries. There are occasionally some organs touched or connected, which require separation. The touched organs can be separated by a combination of RE and GI as was mentioned earlier. Then they can be recognized based upon their gravity center and sizes (along the x, y, and z axis). See Table 1 and 2 for size and position data, respectively, of left kidney, spleen, and stomach. Then for an observed gravity center position  $P_x, P_y$ , and  $P_z$  and sizes  $S_x, S_y$ , and  $S_z$  we make a simple statistical decision based upon a likelihood test assuming that these values have a mutually independent Gaussian distribution.

Table 3 lists the final recognition result where 'O' shows correct recognition, 'X' shows incorrect recognition, and '-' shows a missing organ due to the fact that the organ was already removed by surgery. Since there are 34 organs in the four CT data and the number of correctly recognized organs is 31, we have a recognition accuracy of 91%. The reason for incorrect decision is largely attributed to the fact that CT#1 and CT#4 do not contain a sufficient amount of dye.

Table 3: Organ Recognition Result

Organs	#1	#2	#3	#4
Spine	o	o	o	o
Ribs	o	o	o	o
P.Artery	o	o	o	o
Vena Cava	x	o	o	x
R.Kidney	o	o	-	o
L.Kidney	o	o	o	-
Spleen	o	o	o	o
Stomach	x	o	o	-
Liver	o	o	o	o

## 6 Conclusion

It is found that 3D morphological operations are very useful for our recognition task. Extraction is largely done by conditional dilation and DTT to remove noise and to extract bright regions. A combination of RE and GI is found to be very effective for separating touched organs. Recognition was carried out by a simple maximum likelihood test with organs' positions and sizes.

As our future work, we would like to include more CT data in order to gather more reliable statistics.

## References

- [1] H.Sekiguchi, K.Sano and T.Yokoyama, "Interactive 3-Dimensional Segmentation Method Based on Region-Growing Method", *The Trans. of IEICE*, Vol. J76-D-II, No. 2, pp.350-358, Feb. 1993.
- [2] T.Saito and J.Toriwaki, "A sequential thinning algorithm for three dimensional digital pictures using the euclidean distance transformation", *The 9th Scandinavian Conference on Image Analysis*, pp.507-516. June 1994.
- [3] Y. F. Tsao and K. S. Fu, "A parallel thinning algorithm for 3-D pictures" *COMPUTER GRAPHICS AND IMAGE PROCESSING*, Vol. 17, pp.315-331, 1981.
- [4] F.Meyer: Contrast Feature Extraction, *Quantitative Analysis of Micro-structures in Material Sciences, Biology and Medicine*, J.-L. Chermant, ed., Special issue of *Practical Metallography*, Riederer Verlag, Stuttgart, Germany (1978).
- [5] L.Gu, N.Tanaka, T.Kaneko, R.M.Haralick. "The Extraction of Characters from Cover Images Using Mathematical Morphology", *The Trans. of IEICE D-II* Vol.J80 NO.10, pp.2696-2704, Oct. 1997.
- [6] L.Gu, T.Kaneko, N.Tanaka, "Morphological Segmentation Applied to Character Extraction from Color Cover Images", *Int'l Symp. on Mathematical Morphology and Its Application to Image and Sig. Proc* June 3-5, 1998, Netherlands, pp.367-374.